Large eddy simulation of turbulent flows around bluff bodies in overlaid grid systems

Yoshiaki ITOH [1] , Tetsuro TAMURA [2]

[1] *Kajima Technical Research Institute, 19-1, Tobitakyu 2-Chome, Chou city, Tokyo, Japan*
[2] *Tokyo Institute of Technology,4259, Nagatsuta, Midori-ku, Yokohama city, Kanagawa, Japan*

ABSTRACT

LES of turbulent flow around a circular cylinder at *Re*=10000, with or without numerical viscosity due to third-order upwind scheme, are carried out. Considerable differences are shown in the wake structures and pressure and velocity distributions between both models.

KEYWORDS: LES, circular cylinder, upwind scheme, Overset grid

1. INTRODUCTION

In order to simulate the complex turbulent flow around bluff bodies at high Reynolds numbers, a Large Eddy Simulation is often carried out with numerical viscosity, which is induced by a high-order upwind scheme of advection terms. Then, it is desirable that the effect of the sub-grid scale model be far superior to numerical dissipation due to the upwind scheme. In the LES of a turbulent flow around a square cylinder, it was pointed out that the usage of the upwind scheme causes the narrow recirculation region of wake [1]. The appropriately small numerical viscosity, avoiding numerical instability, improves the accuracy of LES [2]. In this study, in order to grasp the results predicted by an ideal LES, we try to carry out the LES around a circular cylinder without an upwind scheme at *Re* =10000 ($Re=U_0D/\nu$, U_0: velocity of approaching uniform flow, D : the diameter of a circular cylinder, ν : kinematic viscosity). The effect of numerical viscosity on the flow fields is clarified.

2. COMPUTATIONAL METHOD AND MODEL

The filtered governing equations of the three-dimensional incompressible viscous flow are transformed into a generalized coordinate system (ξ, η, ζ) through the collocated grid system [3]. A subgrid scale model of this LES is the Dynamic Smagorinsky Model (DSM) [4]. Here, negative values of eddy viscosity ν_T are truncated to zero. As the solution algorithm, the fractional step with second order accuracy in time [5] is used. The time integration technique of pressure gradient terms and the viscous terms are the Crank-Nicolson scheme. For the advection term, the third-order Adams-Bashforth scheme is adopted. Concerning the spatial discritization, the advection term is approximated using the 4th-order interpolation-method [6] and the 3rd-order upwind scheme as follows:

$$JU\frac{\partial u}{\partial \xi} = \overline{JU\frac{\delta u}{\delta \xi}}\bigg|_i + \alpha J|U|\frac{u_{i-2}-4u_{i-1}+6u_i-4u_{i+1}+u_{i+2}}{12\Delta\xi} \qquad (1)$$

$$\frac{\delta f}{\delta \xi}\bigg|_i = \frac{f_{i-3/2}-27f_{i-1/2}+27f_{i+1/2}-f_{i+3/2}}{24}, \quad \overline{\phi}\big|_i = \frac{-\phi_{i-3/2}+9\phi_{i-1/2}+9\phi_{i+1/2}-\phi_{i+3/2}}{16} \qquad (2), (3)$$

Here, J, U, u, α, and i respectively mean Jacobian, the contravariant velocity in the ξ direction, a velocity in x-direction, the coefficient of numerical viscosity, and grid number in ξ direction. The pressure gradient term at a cell center is approximated using the 4th-order central finite difference method. Other spatial derivatives are approximated using a second order central finite difference scheme. In this study the numerical viscosity is introduced as the condition of α=0.5 , which is equivalent to half the UTOPIA scheme or one sixth of the Kawamura-Kuwahara scheme.

In this study, the overlaid grid technique [7] as shown in Fig.1(a) is adopted for the O-type Boundary-Fitted Coordinate system (number of grid points: ξ , η ,ζ=300, 30, 30 points) and the Cartesian grid system. The length of the whole computational region and the number of grid points in the Cartesian grid are shown in Table.1. The original of the grid system is the center

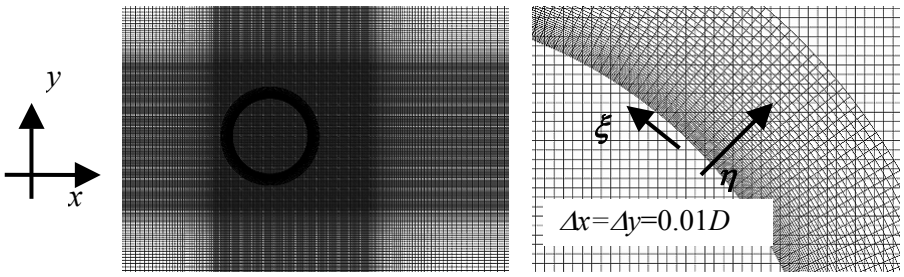

Table.1 Properties of Cartesian grid

Coordinate direction	Length	Number of grid points
x	18.5D	361
y	22.2D	361
z	2D	30

(a) Cartesian grid system and boundary-fitted coordinate system (b) Around the surface of a circular cylinder

Figs.1 Overlaid grid systems

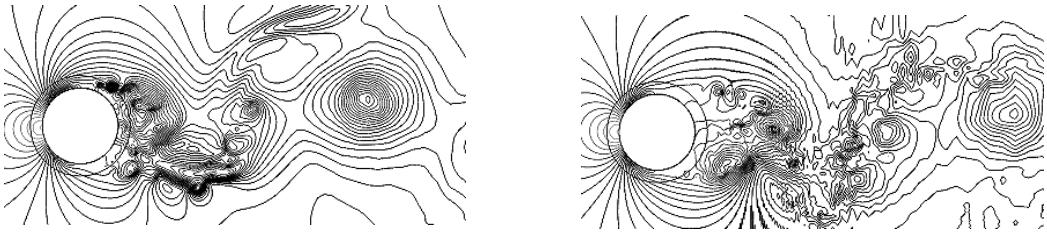

(a) UPW model (b) CNT model

Figs.2 Instantaneous pressure contour around a circular cylinder in a central spanwise direction

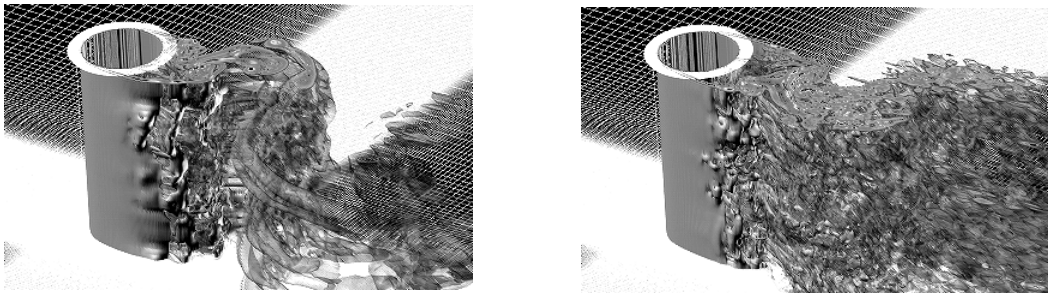

(a) UPW model (b) CNT model

Figs.3 Instantaneous vorticity isosurfaces around a circular cylinder at Re=10000

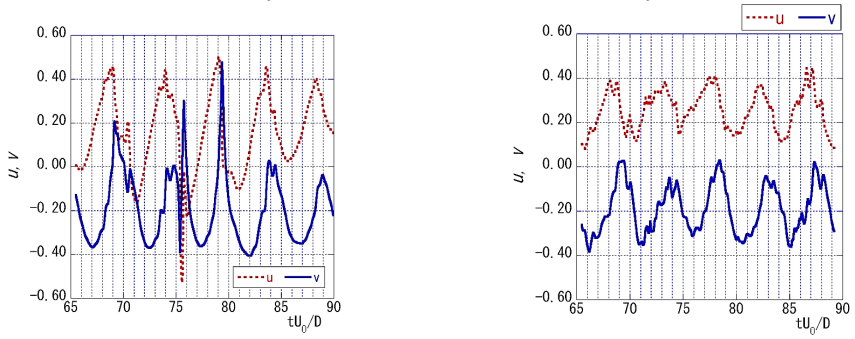

s

(a) 4th-order CNT model (b) 3rd-order UPW model

Figs.4 Time histories of wind velocity in the wakes of a circular cylinder at Re=10000

Table.2 Aerodynamic Properties

Model name	Re	CD_{ave}	CD_{std}	CL_{std}	Cpb_{ave}	St
UPW	10000	1.263	0.077	0.576	-1.382	0.195
CNT	10000	1.135	0.037	0.325	-1.162	0.220
DNS[11]	10000	1.143	*	0.448	-1.129	0.203
Exp.[8]	32000	1.230	*	*	-1.270	0.191
Exp.[9]	9700-9950	*	0.096	0.463	*	*

of a circular cylinder. The reduced time increment ($\Delta tU_0/D$) is equal to 0.00005. The model name of α=0.5 is called 'UPW'. The model name of α=0.0 is called 'CNT'.

3. DIFFERENCE IN WAKE STRUCTURES BETWEEN UPW AND CNT MODELS

Firstly, the instantaneous pressure contours around a circular cylinder are shown in Figs. 2. The wake structures behind a circular cylinder in the case of the CNT model can be captured, though numerical oscillation is partially visible unlike the UPW model. In order to grasp the difference in wake structures between the UPW and CNT models, the instantaneous three-dimensional isosurfaces of vorticity ($=(\omega_x+\omega_y+\omega_z)^{1/2}$) are shown in Figs. 3. When examining spanwise variations of the separated shear layers and the scale of vortices behind a circular cylinder, the wake structures of the CNT model are much smaller than those of the UPW model. It is characteristic that the streamwise vortices behind the cylinder of the UPW model can be clearly observed. The difference in flow structures between the CNT and UPW models affects the time variation in $(u-U_0)/U_0$ and v/U_0 at the point of x=1.12D and y=0.8D, as shown in Figs.4. In the case of the UPW model an abrupt change of v from tU_0/D=75-77 can be observed due to the passing of streamwise vortices. On the other hand, in the case of the CNT model, the time variations are periodic and contain a lot of components of higher frequency than the Strouhal component because of the coherent wake structures formed by the gathering of small vortices.

4. NUMERICAL VALIDATION

In order to evaluate the numerical accuracy of both the UPW and CNT models, this computational aerodynamics are compared with the previous experimental [8-10] and computational [11] results, as shown in Table. 2. The results of the UPW model are a little closer to the experimental results in comparison with those of the CNT model. In order to check the detail, the pressure distributions around the cylinder and the distributions of streamwise velocity along the centerline of the cylinder are respectively shown in Figs. 5 and 6. The time-averaged pressure distributions in the CNT model are quantitatively coincident with the DNS result and are qualitatively the same as the experimental result. The base pressure(θ =180^o) in the case of the UPW model becomes quite low. Taking into consideration the fact that the recirculation region of the UPW model is smaller than the experimental results, as shown in Fig. 6, in the case of the UPW model, it is considered that the effect of the upwind scheme clearly observed [1]. In the case of CNT the scale of recirculation is coincident with the experimental results, though the reverse flow velocity is smaller than that of the experiments as shown in Fig. 6. The fluctuating pressure distributions around the cylinder in the case of the CNT model are closer to the experimental ones from θ =0^o to θ =80^o , as shown in Fig. 5(b). Taking into consideration the fact that the small computational domain in a spanwise direction represses the fluctuation of flow, the results of the CNT model are expected to approach the experimental results in the case of a larger spanwise domain [12].

5. DISTRIBUTIONS OF TURBULENT EDDY VISCOSITY

In order to investigate the contribution of the DSM, the ratio ($\nu_T+\nu$)/ν of eddy viscosity (ν_T) to kinematic viscosity (ν) is shown in Figs. 7. In the case of the CNT model the regions where the eddy viscosity ν_T is ten times larger than the kinematic viscosity are evenly distributed in the wake of a circular cylinder in comparison with the UPW model. It seems that the presence of numerical viscosity reduce the effect of eddy viscosity.

6. CONCLUSION

The results of LES of turbulent flow around a circular cylinder at Re=10000 without numerical viscosity due to upwind scheme (the CNT model) are compared with those of LES with upwind scheme (the UPW model), the previous experimental and computational results. The flow structures of wakes in the UPW model are larger than those of the CNT model. The results of the CNT model are almost coincident with the experimental data and DNS data.

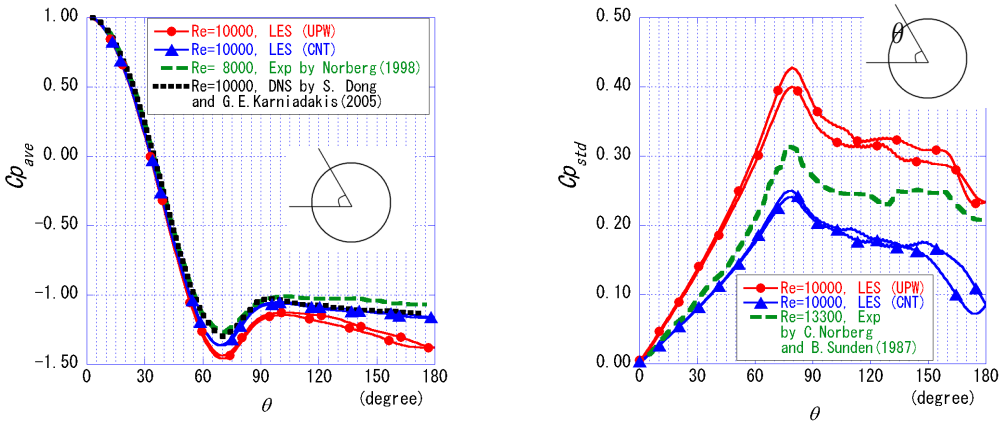

(a) Time mean pressure (b) Fluctuating pressure

Figs.5 Pressure distributions around a circular cylinder at *Re*=10000

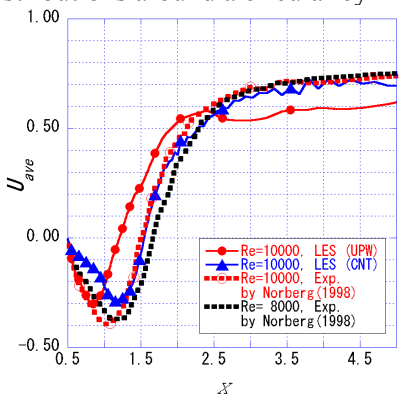

Fig.6 Time mean velocity in streamwise velocity along the centerline of a circular cylinder at *Re*=10000

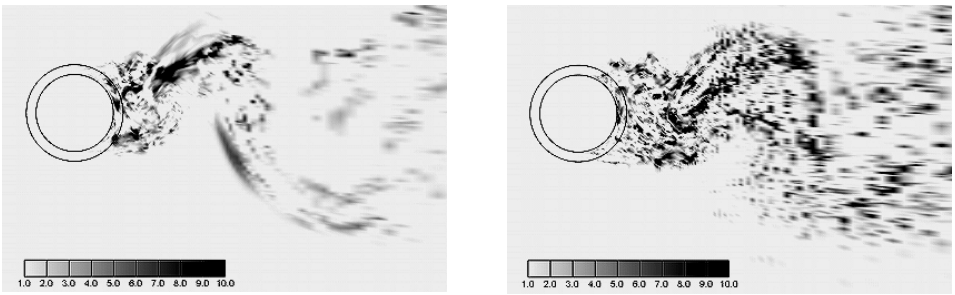

(a) UPW model (b) CNT model

Figs.7 Instantaneous distributions of the ratio $(\nu_T+\nu)/\nu$ around a circular cylinder at *Re*=10000

REFERENCES

[1]W. Rodi, J. H. Ferziger, M. Breuer and M. Pourquie, Status of large-eddy simulation; results of a workshop, J. Fluids Eng., 119 (1997) 248-262 [2] Y. Ono and T. Tamura , Large eddy simulation using a curvilinear coordinate system for th e flow around a square cylinder, 5, 2-4 (2002) 369-378 [3] T. Tamura and T. Kitagishi, Application of the interpolation method in generalized coordinate system to wake flows around a circular cylinder, J. Struct. Constr. Eng., AIJ, 545 (200 1) 27-34 [4]M. Germano, U. Piomelli, P. Moin, and W. Cabot, A dynamic subgrid-scale eddy viscosity model, Phys. Flui ds, A3 (7) (1991) 1760-1765 [5] J. K. Dukowicz and A. S. Dvinsky, Approximation as a higher order splitting for the im plicit incompressible flow equations, J. Comput. Phys., 102 (1992) 336-347 [6]T. Kajishima, High-order finite difference methods for wall-bounded incompressible flows, Proc. 5th Int. Symp. Comp. Fluid, 1993, 414-419 [7] Y. Itoh and R. Hi meno, Numerical investigation on unstable oscillations of two circular cylinders in tandem arrangement, Proc. ASME FE DSM2003 (2003)45460 [8]C. Norberg and B. Sunden, Turbulence and Reynolds number effects on the flow and fluid for ces on a single cylinder in cross flow, J. of Fluid s and Structures 1 (1987) 337-357 [9]G.S. West and C. J. Apelt, Measur ements of Fluctuating pressures and forces on a circular cylinder in the Reynolds number range 10^4 to $2.5x10^5$, J. of Fluid s and Structures , 7 (1993) 227-244 [10]C. Norberg, LDV-measurements in the wake of a circular cylinder, Advances in Understanding of Bluff Body Wakes and Vortex-induced Vibration, Washington DC (1998) 1-12 [11]S. Dong, G. E. Kar niadakis, DNS of flow past a stationary and oscillating cylinder at *Re* =10000, J. of Fluids and Structures 20 (2005) 519-5 31 (2005) [12]M. Kuroda, T. Tamura and M. Suzuki, LES analysis to turbulent wake of rectangular cylinder, Summaries of technical papers of annual meeting AIJ2005 (2005)